Urol Res (2011) 39:245–251
DOI 10.1007/s00240-010-0359-1

ORIGINAL PAPER

Simulating calcium salt precipitation in the nephron using chemical speciation

Allen L. Rodgers · Shameez Allie-Hamdulay · Graham Jackson · Hans-Göran Tiselius

Received: 4 May 2010 / Accepted: 30 December 2010 / Published online: 20 January 2011

Abstract Theoretical modeling of urinary crystallization processes affords opportunities to create and investigate scenarios which would be extremely difficult or impossible to achieve in in vivo experiments. Researchers have previously hypothesized that calcium renal stone formation commences in the nephron. In the present study, concentrations of urinary components and pH ranges in different regions of the nephron were estimated from concentrations in blood combined with a knowledge of the renal handling of individual ions. These were used in the chemical speciation program JESS to determine the nature of the solution complexes in the different regions of the nephron and the saturation index (SI) of the stone-forming salts calcium oxalate (CaOx), brushite (Bru), hydroxyapatite (HAP) and octacalcium phosphate (OCP). The effect of independent precipitation of each of the latter on the SI values of other salts was also investigated. HAP was the only salt which was supersaturated throughout the nephron. All of the other salts were supersaturated only in the middle and distal regions of the collecting duct. Supersaturations were pH sensitive. When precipitation of CaOx, Bru and OCP was simulated in the distal part of the collecting duct, little or no effect on the SI values of the other stone forming salts was observed. However, simulation of HAP precipitation caused all other salts to become unsaturated. This suggests that if HAP precipitates, a pure stone comprising this component will ensue while if any of the other salts precipitates, a mixed CaOx/CaP stone will be formed. Application of Ostwald's Rule of Stages predicts that the mixed stone is likely to be CaOx and Bru. Our modelling demonstrates that precipitation of stone-forming salts in the nephron is highly dependent on the delicate nature of the chemical equilibria which prevail and which are themselves highly dependent on pH and component concentrations.

Keywords Urinary crystallization · Nephron · Chemical speciation · Salt precipitation · Stone formation

A. L. Rodgers (✉) · S. Allie-Hamdulay · G. Jackson
Department of Chemistry, University of Cape Town, Cape Town, South Africa
e-mail: Allen.rodgers@uct.ac.za

H.-G. Tiselius
Department of Urology, Karolinska University Hospital, Stockholm, Sweden

Introduction

In order to understand the fundamental principles of any chemical or physical process, a working model which closely resembles the real situation is required. The closer the resemblance, the more credible are the conclusions. In the case of urolithiasis, understanding the processes which govern the crystallization of salts in urine is fundamental to understanding the original pathogenesis underlying the disease and, as a consequence, the management thereof. Indeed, if the ultimate goal is prophylaxis, then understanding the physicochemical factors which direct or prevent crystallization of calcium oxalate (CaOx) and calcium phosphate (CaP) salts is vital. Facilitation of this basic understanding must be provided by the models which are employed.

In the study of urolithiasis, four fundamental models have been utilized. Clearly, since this is a disease which afflicts humans, the first (and obvious) model is the human body itself. The others are the animal model, the in vitro model and the theoretical or virtual model. Each has advantages and limitations. Each has yielded insights

Table 1 Urine concentrations in different regions of the nephron

Variable (m mol/l)	GF	PT	LH	DTp	DTd	CDm	CDd
Calcium	1.50	2.78	3.47	1.32	0.94	1.60	4.50
Magnesium	0.54	0.19	0.24	0.12	0.40	1.45	3.85
Phosphate	0.80	0.80	1.00	1.00	3.34	12.1	32.3
Oxalate	0.0015	0.01	0.013	0.013	0.04	0.12	0.32
Citrate	0.07	0.09	0.11	0.11	0.37	1.21	3.21
Sodium	135	135	278	79	93	94	109
Chloride	139	139	293	101	145		
Potassium	3.8	3.0	13.8	0.90	58.0	53.0	63.7
Sulfate	1.4	3.1	3.9	3.9	13.0	7.8	20.8
pH	7.40	6.75	6.50–7.30	6.38–7.00	6.45–7.00	5.00–6.25	5.50–6.70

GF Glomerular filtrate, *PT* Proximal tubule, *LH* Loop of Henle, *DTp* Disital tubule proximal, *DTd* Distal tubule distal, *CDm* Collecting duct middle, *CDd* Collecting duct distal

which others have overlooked. Although the human model would seem to be the "best", it suffers from ethical, practical and resource-based challenges. On the other hand, theoretical modelling offers several advantages: it allows the researcher to simulate the human situation to a reasonable extent; it affords wide-ranging opportunities to manipulate the urinary environment and to compute physicochemical risk factors for stone-formation; there are no ethical hurdles which need to be negotiated and labour and cost dependent resources are insignificant.

We have previously employed the software package JESS to model chemical speciation in urine [1] and our findings have recently been confirmed by others [2]. We have also demonstrated that JESS has great versatility, allowing investigators to model precipitation processes among other applications [3].

Researchers have frequently made the point in previous studies that it can be reasonably assumed that the formation of calcium renal stones commences in the nephron and that characterization of the crystallization processes which occur here are key to our understanding the pathogenesis of this disease [4–9]. The present study was undertaken to model these processes.

Methods

Urinary data published by Luptak et al. [4] and Tiselius et al. [9] as well as data provided in private correspondence by HG Tiselius (Karolinska Hospital, Sweden) were used for modelling crystallization in different regions of the nephron (Table 1). These data were obtained from various sources. When data were missing, indirect assumptions were made from concentrations in blood combined with knowledge of the renal handling of the individual ion. Calcium concentration was estimated using the value reported by Luptak et al. [4]. The estimation took into account a volume reduction in the proximal tubules of 80% and a re-absorption of calcium of 63%. Values in Table 1 represent the mean of 24 h urine data derived from different sources and from logical calculation and inter- and extrapolations. This approach was necessary to constitute our model, since empirical concentration values are very scanty. The Joint Expert Speciation System (JESS) (Mayhem Unit Trust and Council for Scientific and Industrial Research, Pretoria, South Africa) was used to calculate speciation and to model crystallization [10, 11]. Within this package, the saturation index, scanning and precipitation applications were utilized. The saturation index (SI) is equivalent to the relative supersaturation (RS). It is calculated according to the same physicochemical principles as RS values generated by EQUIL [12], but utilizes a more extensive database containing calcium phosphate species which are not present in EQUIL and which consequently affect the ultimate value of the relative supersaturation of CaOx [1, 2]. Like EQUIL, JESS does not consider the effect of crystal size on solubility. According to the Kelvin-Ostwald-Freundlich Effect, the solubility of crystals increases when their size drops below 1 μm. Since solubilities are routinely assessed using crystals which are bigger than this threshold, experimental values will underestimate the value as it exists in a nucleating system. Thus, supersaturation values which are calculated by EQUIL and JESS using these solubilities, might possibly represent overestimations of the true values. For the scanning option, JESS allows selected parameters to be systematically varied ("scanned") within specified ranges and then calculates the resultant speciation and concomitant SI values. For the precipitation option, JESS allows a selected supersaturated salt to precipitate until equilibrium is established and then calculates the effect on the SI values of the salts which have remained in solution.

Results

SI values for CaOx and brushite (Bru) in the different regions of the nephron and at different pH levels are shown in Figs. 1, 2, respectively. Because SI values for hydroxyapatite (HAP) and octacalcium phosphate (OCP)

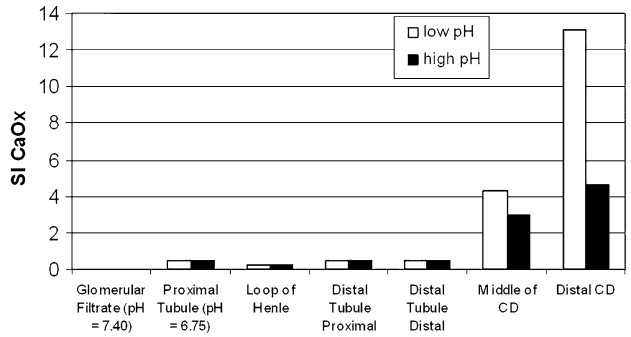

Fig. 1 SI values for CaOx in the different regions of the nephron and at different pH levels

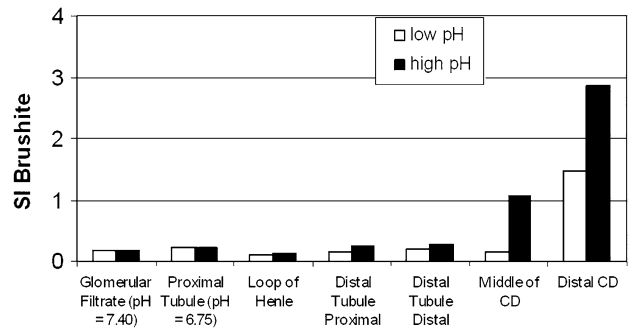

Fig. 2 SI values for brushite in the different regions of the nephron and at different pH levels

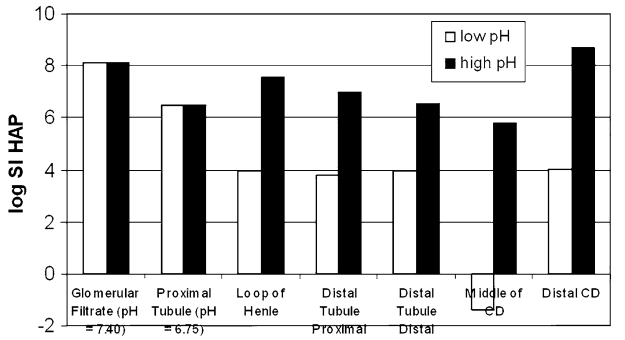

Fig. 3 Log SI values for hydroxyapatite (HAP) in the different regions of the nephron and at different pH levels

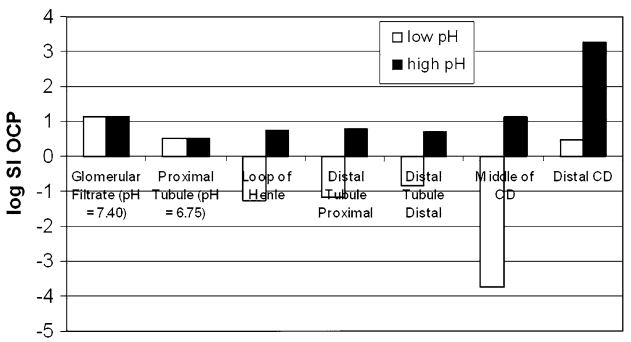

Fig. 4 Log SI values for octacalcium phosphate (OCP) in the different regions of the nephron and at different pH levels

vary by several orders of magnitude in the different parts of the nephron, it is more convenient to plot the log function for these salts (Figs. 3, 4, respectively). It is noted that there is a general sequential increase in SI values for CaOx, Bru and OCP from the loop of Henle, through the proximal and distal regions of the distal tubule and finally through the mid and distal regions of the collecting duct. Values for HAP show a decrease from the loop of Henle to the middle of the collecting duct, but then increase in the distal part of the collecting duct. Another feature worth noting are the low saturation levels of CaOx, Bru and OCP in the loop of Henle compared to HAP levels which are very high. Also of interest is that for CaOx, values in the loop of Henle and the distal tubule were not affected by pH but values decreased with increasing pH in the collecting duct. On the other hand, values for the three calcium phosphate salts increased in all regions with increasing pH. The only salt which is supersaturated (SI $>$ 1 or log SI $>$ 0) throughout the nephron at low and high pH values is HAP (except in the middle of the collecting duct at low pH). All of the other salts are supersaturated only in the middle and distal parts of the collecting duct. This observation is consistent at the high end of the pH range. However, at the lower end, Bru (middle of collecting duct) and OCP (middle and distal collecting duct) are unsaturated.

The presence of supersaturated salts at the lower end of the respective pH ranges in the different regions of the nephron is summarized in Fig. 5.

It is important to recognize that we are presenting here a model of the risk of crystallization in different parts of the nephron. SI values were calculated on the basis of estimated values, as opposed to measured values. Therefore, there are no standard deviations. As such, calculations of the statistical significance between SI values cannot be performed. Since there are no errors in the calculations per se, the SI differences shown in Figs. 1, 2, 3, 4 represent differences in the physicochemical risk of crystallization. Since these differences may be clinically significant, our results are worth noting.

The consequences of modeling the independent precipitation of CaOx, HAP, OCP and Bru in the distal part of the collecting duct, at the low and high ends of the pH range in this region, are shown in Fig. 6a, b, respectively. As mentioned previously, log SI values are plotted because SI for the different salts vary by several orders of magnitude. It is observed that when any one of CaOx, OCP or Bru precipitates at the lower pH (Fig. 6a), log SI values of the non-precipitating salts remain $>$1 (except for OCP during precipitation of Bru), indicating that supersaturation of

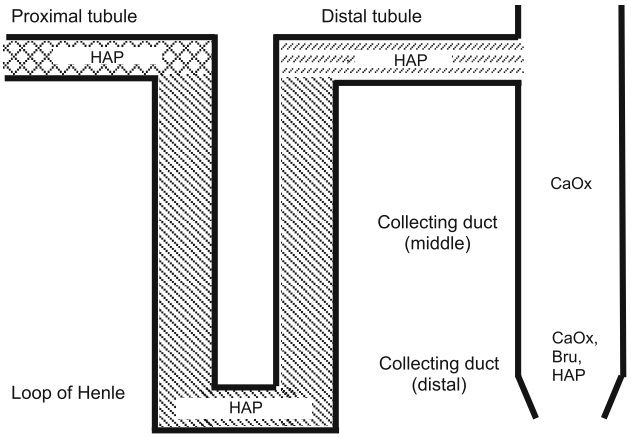

Fig. 5 Supersaturated salts in the different regions of the nephron at the lower end of the respective pH ranges

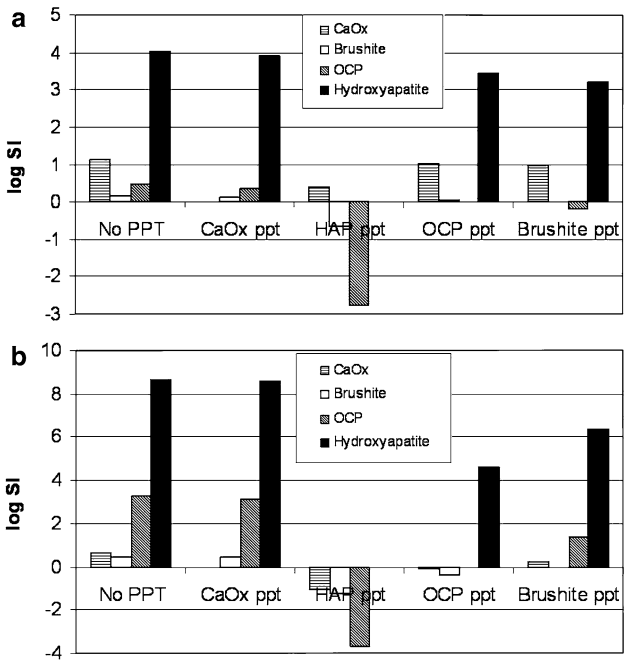

Fig. 6 **a** Effect of precipitation on log SI values of each salt in the distal region of the collecting duct at the lower end of the pH range. **b** Effect of precipitation on log SI values of each salt in the distal region of the collecting duct at the upper end of the pH range

these salts is retained. However, when HAP precipitates (Fig. 6a) the SI value for CaOx decreases significantly while those for Bru and OCP decrease to below unity, indicating that these salts are no longer in a saturated state. At the higher pH, precipitation of CaOx has no effect on the SI values of the other salts while individual precipitation of OCP, Bru and HAP causes the SI values of the other salts to decrease (Fig. 6b). The most dramatic effect occurs when HAP precipitates, as all of the other salts become unsaturated.

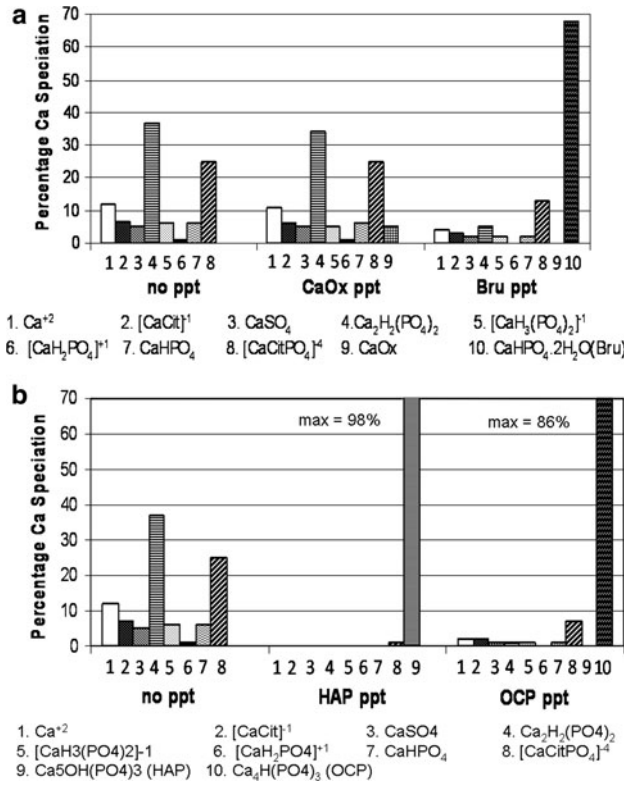

Fig. 7 **a** Percentage distribution of Ca speciation in the distal region of the collecting duct after independent precipitation of CaOx and Bru. **b** Percentage distribution of Ca speciation in the distal region of the collecting duct after independent precipitation of HAP and OCP

These effects can be explained by consideration of changes in the percentage distribution of the numerous Ca species during the precipitation of each salt. The distributions at the high end of the pH range are shown in Fig. 7a after precipitation of CaOx and Bru and in Fig. 7b after precipitation of HAP and OCP. It is noted that when CaOx precipitates, the percentage of each of the various Ca species is hardly affected. On the other hand, precipitation of Bru or OCP utilizes sufficient Ca to cause small decreases in the distribution, thereby inducing small concomitant decreases in the SI of each of the Ca salts. However, when HAP precipitates, it utilizes 99% of the available Ca, causing a dramatic decrease in the formation of all of the other Ca salts and their SI values.

Discussion

Compelling theoretical and in vitro empirical evidence has been provided by several authors which suggests that the initial step in calcium stone formation may involve precipitation of calcium phosphate (CaP) in the nephron above the collecting duct, which initiates either heterogeneous

nucleation of CaOx or a pH dependent dissolution of CaP in which Ca is released thereby causing precipitation of CaOx. In most cases, the species "CaP" has not been defined. However, in other cases, authors have referred to Bru, HAP, OCP and ACP in different parts of the nephron [4, 9, 13]. Our results provide now, for the first time, a consolidated overview of the different supersaturated Ca salts occurring over a range of different pH values in LH, DTp, DTd, CDm and CDd. The presence of supersaturated Bru and HAP in the distal tubule over the entire predicted pH range supports the notion of the possible precipitation of "CaP" in the nephron above the collecting duct while the potential for a pH dependent dissolution is also demonstrated with respect to OCP, which becomes unsaturated if the pH drops in this region.

In demonstrating the relative risk of crystal formation in the different regions of the nephron, we recognize that peaks and troughs of supersaturation occur as a consequence of diurnal and individual variations in dietary and metabolic determinants.These extremes occur transiently but can be decisive. In some situations, metastable fluid can pass through the nephrons without mineralization occurring during the transit time, while under other conditions, crystallization in the same metastable fluid can occur. These daily variations have the strongest effect in the latter parts of the nephron where the fine tuning for most body equilibria is performed.

It is also important to recognize that the passage of urine through the different regions of the nephron is accompanied by many dynamic processes which constantly alter the supersaturation of salts and their risk of crystallization. For example in the descending part of a loop of Henle, water is taken up almost exclusively and salts are retained in the fluid. In the ascending part, these processes are reversed as no water is taken up and salts are reabsorbed. The net effect is that the conditions at the end of the proximal tubule and the beginning of the distal tubule are fairly similar. However, the main difference is the net removal of water, which manifests itself as a net increase in the concentration of all compounds that are not reabsorbed in the loops, like oxalate.

Similarly, variations in pH affect the risk of crystallization. As indicated in Table 1, the pH range in the Loop of Henle is from 6.5 to 7.3. These values represent the natural variation in the length of the loops, corresponding to those expected at the tips of short and long loops, respectively [6, 14, 15]. In the descending part, water is reabsorbed and some CO_2 passively diffuses out of the fluid. The net result is that the equilibrium $CO_2 + H_2O \leftrightarrow HCO_3^- + H^+$ shifts to the left, thereby causing an increase in pH. Diffusion (and hence pH) increases as the length of the loop increases. Most nephrons have short loops where the pH will not increase above 7.0, thereby implying that there will be no risk for nucleation of phosphate salts. However, in nephrons having long loops, the pH may reach 7.4 (as measured in micropuncture studies). In these loops the drive to nucleate phosphate salts is high. The number of nephrons with long loops differs between individuals and is also related to age [8]. Interestingly, the number of long loops is lowest in children and the elderly, corresponding to those groups in which the occurrence of stone formation is lowest.

Furthermore, our modelling of precipitation processes in CDd provides insights into new mechanisms by which pure and mixed Ca stone formation may occur. These are based on the observations that SI values of all of the complexes decreased to below supersaturation levels when HAP was allowed to precipitate (except CaOx at the low end of the pH range where a significant decrease nevertheless occurred), but did not change at all when CaOx precipitated, and changed by very little when Bru precipitated. The implications are that if HAP precipitates in CDd, it is likely that a pure stone comprising only this component will form, while if CaOx or Bru precipitates, a mixed CaOx/CaP stone is a possible outcome. However, in making these predictions, it needs to be recognized that kinetic factors have not been incorporated into the modeling. Like EQUIL, JESS invokes thermodynamic principles only. Because the kinetics of complexation and saturation of inorganic salts are very fast, while the kinetics of their precipitation is relatively slow, kinetic factors are likely to produce effects on SI values which lie between the extremes of no precipitation and precipitation, shown in Fig. 7.

Application of Ostwald's Rule of stages [16–18] in the present model yields interesting insights into the preferred sequence in which the saturated urinary salts are likely to precipitate. This rule was constructed to explain the peculiar finding that the first mineral formed is not necessarily the one that is thermodynamically most favoured. It is determined by the difference in free energy of the ions in solution versus those in the solid state. However, the ions that will form the eventual crystal are not present as free entities in the solution. Each will be surrounded by a mantle of other compounds through small attracting forces. This might comprise, for example, a water mantle with possible inclusion of sodium and chloride ions. The probability for the initial ion-pair collision and crystal formation will then depend on their concentrations and on the energy required to penetrate this mantle. Formation of the ion pair complex requiring the least input of energy will be favoured. Thus, when calcium and oxalate ions combine, the preferred route is through COT where the arrangement in the crystal lattice most resembles the fluid conditions. As is well known, COT is not stable. As such, it is hardly, if ever, observed in a stone. For calcium phosphates, similar short-lived crystal types exist which will be formed first.

They are not recovered in the final stone but they do dictate the rate at which a solid is formed. The thermodynamic drive needed to form these initial phases is lower than the drive calculated from the solubility of the more stable end-products. Thus, the first solid to precipitate in a sequence of precipitating solids is that which is least supersaturated. In the present study, Bru has the lowest SI value of the supersaturated salts. Thus of the different precipitation scenarios described above, a mixed stone is predicted by the present urinary model. Since CaOx will be the least supersaturated salt after precipitation of Bru, the composition of the mixed stone is likely to be Bru/CaOx. Although the latter type of stone is a relatively rare clinical occurrence, the dependence of stone formation on delicate speciation equilibria is apparent.

Of interest is that the formation of a pure CaOx stone is not predicted by the present model. Application of Ostwald's rule indicates that a pure CaOx stone would form if its SI is less than that of Bru. This, in turn, is dependent on the speciation which has its own dependence on pH and other urinary factors. Since we believe that our model of urinary concentrations is reasonably accurate, we suggest that the absence of a pure CaOx stone in the present model again bears testimony to the fragile nature of the chemical equilibria which exist in CDd (and elsewhere in the nephron). These equilibria depend on multiple factors among which are the presence or absence of macromolecular modifiers of CaOx and Bru crystallization. Like EQUIL and all other speciation computer programs, JESS is unable to simulate the effects of such modifiers. Their absence from the model may therefore have dictated the absence of a pure CaOx stone. On the other hand, it may be argued that JESS is quite correct in predicting that the formation of a chemically pure CaOx stone in which there is 0% of any other component such as CaP, is unlikely. Powerful modern physicochemical techniques may yet confirm this hypothesis.

Despite our findings, pathological crystallization needs to be considered in a wider perspective in view of the recent observations on the origin of CaOx stones involving apatitic Randall's plaque [19, 20]. Initial crystal formation in the nephron might result in solid phases that either remain intratubular or become internalized and processed by the tubular cells. Accordingly, it is likely that the apatite crystal mass forming Randall's plaques have their origin in the long loops of Henle from where they are transported to a subepithelial position—either intact or possibly following dissolution and re-crystallization in the interstitial tissue. Whether the subepithelial apatite accumulations (Randall's plaques) are the dominant cause of CaOx stone formation as suggested by Evan and coworkers [19, 20] remains to be shown, but intratubular deposits at the end of the collecting tubules (Ducts of Bellini) have been demonstrated in both humans and animals [21, 22].

The results presented in this paper are totally dependent on the model (i.e., urine concentrations in the different regions of the nephron) which was used for the calculations. Of course, a different model is likely to predict different risk profiles. However, we believe that the model which we employed in the present study, and the results which it generated, are sufficiently credible to stimulate insightful discussion and debate about the mechanisms by which calcium stone formation might be initiated in the nephron.

Acknowledgments The authors are grateful to the South African National Research Foundation (NRF), the Swedish International Development Cooperation Agency (Sida), the South African Medical Research Council and the University of Cape Town for their financial support.

References

1. Rodgers A, Allie-Hamdulay S, Jackson G (2006) Therapeutic action of citrate in urolithiasis explained by chemical speciation: increase in pH is the determinant factor. Nephrol Dial Transpl 21:361–369
2. Pak CYC, Maalouf NM, Rodgers K, Poindexter JR (2009) Comparison of semi-empirical and computer derived methods for estimating urinary saturation of calcium oxalate. J Urol 182:2951–2956
3. Rodgers A, Allie-Hamdulay S, Jackson G (2007) JESS: what can it teach us? In: Evan AP, Lingeman JE, Williams JC (eds) Renal Stone Disease: Proceedings of the First International Urolithiasis Research Symposium, American Institute of Physics, Melville, NY, pp 183–191
4. Luptak J, Bek-Jensen H, Fornander AM, Hojgaard I, Nilsson MA, Tiselius HG (1994) Crystallization of calcium oxalate and calcium phosphate at supersaturation levels corresponding to those in different parts of the nephron. Scanning Microsc 8:47–62
5. Kok DJ (1996) Crystallization and stone formation inside the nephron. Scanning Microsc 10:471–486
6. Kok DJ (1997) Intratubular crystallization events. World J Urol 15:219–228
7. Tiselius H-G (1997) Estimated levels of supersaturation with calcium phosphate and calcium oxalate in the distal tubule. Urol Res 25:153–159
8. Kok DJ, Schell-Feith (1999) Risk factors for crystallization in the nephron: the role of renal development. J Am Soc Nephrol 10:S364–S370
9. Tiselius H-G, Lindbäck B, Fornander AM, Nilsson MA (2009) Studies on the role of calcium phosphate in the process of calcium oxalate crystal formation. Urol Res 37:181–192
10. May P, Murray K (1991) JESS, a joint expert speciation system-I. Talanta 38:1409–1417
11. May P, Murray K (1991) JESS, a joint expert speciation system-II. The thermodynamic database. Talanta 38:1419–1426
12. Werness PG, Brown CM, Smith LH, Finlayson B (1985) EQUIL 2: A basic computer program for the calculation of urinary saturation. J Urol 134:1242–1244
13. Asplin JR, Mandel NS, Coe FL (1996) Evidence of calcium phosphate supersaturation in the loop of Henle. Am J Physiol 270(4 pt 2):F604–F613

14. Kok DJ (1990) Free and fixed particle mechanism—a review. Scanning Micros 471–486
15. Kok DJ, Khan SR (1994) Calcium oxalate nephrolithiasis, a free or fixed particle disease. Kidney Int 46:847–854
16. Ostwald W (1897) Studien uber die bildung und unwandlung fester korper Zeitschrift fur Physikalische. Chemie 22:289–330
17. Threlfall T (2003) Structural and thermodynamic explanations of Ostwald's rule. Org Process Res Dev 7:1017–1027
18. Nyvlt J (2006) The Ostwald Rule of Stages. Cryst Res Technol 30:443–449
19. Evan A, Lingeman J, Coe FL, Worcester E (2006) Randall's plaque: pathogenesis and role in calcium oxalate nephrolithiasis. Kidney Int 69:1313–1316
20. Evan AP, Coe FL, Lingeman JE, Shao Y, Sommer AJ, Bledsoe SB, Anderson JC, Worcester EM (2007) Mechanism of formation of human calcium oxalate renal stones on Randall's plaque. Anat Rec 290:1315–1323
21. Varvaet BA, Verhulst A, De Broe ME, D'Haese PC (2010) The tubular epithelium in the initiation and course of intratubular nephrocalcinosis. Urol Res 38:249–256
22. Fasano JM, Khan SR (2001) Intratubular crystallization of calcium oxalate in the presence of membrane vesicles: an in vitro study. Kidney Int 59:169–178